

First steps toward the generation of PET/MR attenuation map in the case of prostate cancer

Jorge Zavala Bojorquez, Stéphanie Bricq, Paul Walker, Alain Lalande

► **To cite this version:**

Jorge Zavala Bojorquez, Stéphanie Bricq, Paul Walker, Alain Lalande. First steps toward the generation of PET/MR attenuation map in the case of prostate cancer. Journées RITS 2015, Mar 2015, Dourdan, France. p160-161. inserm-01144521

HAL Id: inserm-01144521

<https://www.hal.inserm.fr/inserm-01144521>

Submitted on 21 Apr 2015

HAL is a multi-disciplinary open access archive for the deposit and dissemination of scientific research documents, whether they are published or not. The documents may come from teaching and research institutions in France or abroad, or from public or private research centers.

L'archive ouverte pluridisciplinaire **HAL**, est destinée au dépôt et à la diffusion de documents scientifiques de niveau recherche, publiés ou non, émanant des établissements d'enseignement et de recherche français ou étrangers, des laboratoires publics ou privés.



First steps toward the generation of PET/MR attenuation map in the case of prostate cancer

Jorge Zavala Bojorquez¹, Stéphanie Bricq¹, Paul M. Walker¹, Alain Lalande^{1*}

¹Le2I (UMR CNRS 6306), Faculté de Médecine, Université de Bourgogne, Dijon, France.

*Corresponding author: alain.lalande@u-bourgogne.fr.

Abstract –A new methodology providing the first step towards the generation of attenuation maps for PET/MR systems based solely on MR information is presented in this paper. From T1- and T2-weighted MR data set and anatomical-based knowledge, our method segments and classifies the attenuation-differing regions of the patient's pelvis using a robust implementation of the weighted fuzzy C-means algorithm. Providing no signal, particular process is performed for the bones. We have demonstrated the feasibility of this approach by correctly segmenting and classifying six attenuation-differing regions on images at the level of the pelvis: fat, muscle, prostate, air, background and bones.

Index terms - Image Processing, Magnetic Resonance Imaging.

I. INTRODUCTION

Prostate cancer is the most commonly diagnosed cancer and a leading cause of cancer death worldwide. Magnetic Resonance Imaging (MRI) is currently the imaging modality of choice for visualization, diagnostic and evaluation of prostate cancer. However, on the MR images it is relatively difficult to detect cancer spread to the lymph nodes and the bones. The Positron Emission Tomography / Computer Tomography (PET/CT) is considered as the gold standard for this end. This will change with the arrival of hybrid PET/MR systems and the advantages that MR represents in contrast to CT [1]. Nevertheless, the change cannot take place if an accurate method to generate the photon attenuation maps used for the reconstruction of PET images from MR information is not designed. We propose a robust and automatic method based on the intrinsic parameters T1- and T2-relaxation times of tissues and anatomical-knowledge to create accurate attenuation maps at the level of the pelvis with six regions: fat, muscle, prostate, air, background and bones. To the best of our knowledge, most of these studies have been applied in brain and thorax imaging and little efforts have been done to create accurate attenuation maps for prostate imaging. Our method does not require special sequences to extract bones neither depend on voxel intensities, therefore, is scanner independent and can be implemented in any system.

II. MATERIALS AND METHODS

II.1. T1 and T2 measurements

The images were acquired with a 3T Trio TIM clinical scanner (Siemens Medical Solutions, Germany). Two healthy volunteers (22 and 42 years old) participated in this study after they gave informed consent. Four axial slices were acquired for both T1 and T2 measurements with the same field of view, resolution and position at the high of the pelvis in order to avoid registration between T1 and T2 images (Figure 1).

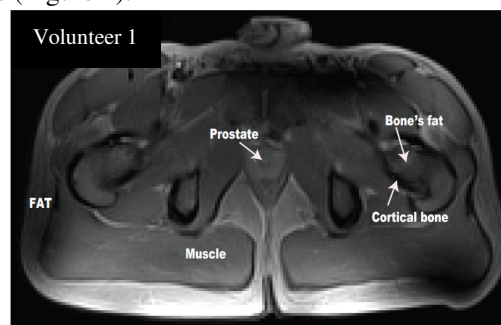


Figure 1: Example of an axial slice at the level of the pelvis.

An inversion recovery-prepared turbo spin echo (TSE) was acquired at eight inversion times (TI: 50, 200, 400, 700, 1200, 2000, 5000, 7860 ms) to obtain the T1-weighted images. The TI were chosen to assure maximum contrast among tissues and to cover the whole span of T1 relaxation times of tissues present in the slice section. The transverse relaxation time T2 was measured using a 32-echo spin echo sequence acquired with TE from 8.8 to 281.6 ms in 8.8 ms steps (TR = 5000 ms). The T1 and T2 were calculated from a magnitude monoexponential fit to the signal recovery data for each voxel using the bisquare nonlinear least squares fitting. For T1, a three-parameter model was used with T1, the equilibrium magnetization S_0 and the inversion efficiency α (variable fitting parameters):

$$S(TI) = |S_0(1 - \alpha e^{-TI/T_1})|$$

The used of a long TR ($> 5 \times T_1$ of the longest T1 of the tissues) allowed the fit of the equation, since the longitudinal magnetization fully recovers before another repetition of the sequence. For T2, a three parameter model was used with T2, the equilibrium magnetization S_0 and the y-offset C as fitting parameters:

$$S(TE) = S_0 e^{TE/T_2} + C$$

To automatically extract the background, we kept the region with the highest number of voxels on the binary image obtained from the longest T1 image with a threshold of 4% of highest voxel intensity. The obtained maps are showed on the figure 2.

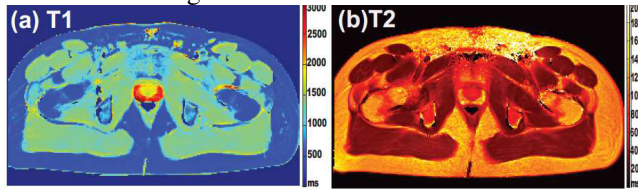


Figure 2: T1 and T2 maps for volunteer 2.

II.2. Segmentation and classification

Segmentation was performed using weighted Fuzzy C-means (wFCM) [2]. The method performs a fuzzy partition and takes as inputs the T1 and T2 maps, the number of clusters ($c=100$ to do firstly an oversegmentation), the fuzzification constant ($m=2$) and the weights. To define these weights, the measure adopted here was entropy, to take advantage of the good spatial resolution of MR images, and because it permits to estimate the randomness of the information which is a common reference in both maps. The centers of clusters were biased towards these measures:

$$\tilde{w}_{kT_1, T_2} = \left(-\sum_{k=1}^K p_{T_1}(T_{1k}) \log p_{T_1}(T_{1k}) \right) \left(-\sum_{k=1}^K p_{T_2}(T_{2k}) \log p_{T_2}(T_{2k}) \right)$$

where p_T represent the probabilities of the different measures T1 or T2. T1 and T2 values were normalized to avoid bias. The centroid values of each cluster were compared with the references T1 and T2 values of the tissues using the euclidean norm for a two dimensional point:

$$d(ce, T_{ref}) = \sqrt{(ce_{T_1} - T_{1_{ref}})^2 + (ce_{T_2} - T_{2_{ref}})^2}$$

where ce represents T1 and T2 values of the centroids, T_{ref} are those of the reference tissues. These reference values were calculated from the average values of different regions of interest, set on the T1 and T2 maps of volunteer 1 for the tissues: fat ($T_1 = 405 \pm 34$ ms, $T_2 = 147 \pm 20$ ms), muscle ($T_1 = 1290 \pm 83$ ms, $T_2 = 39 \pm 3$ ms) and prostate ($T_1 = 1742 \pm 175$ ms, $T_2 = 75 \pm 34$ ms). For air, zero values were used for both T1 and T2 relaxation times. However cortical bone does not produce signal with conventional spin echo sequences used in clinical practice. To detect bones, firstly, the fat's regions are localized. Then a morphological opening operation is performed to remove small regions and narrow segments of fat connecting big regions. Regions in contact with the background are removed and regions having an area smaller than a predefined threshold (100 mm^2) are discarded. For bones, the boundaries of the fat's regions are surrounded by cortical bone, but since this tissue produces no signal with the sequences implemented, it is labeled as air. Therefore, the boundaries of the fat's regions are localized thanks to a dilation with a kernel size of 5×5 , and their labels analyzed.

If the labels do not correspond to an area of at least 22.5 mm^2 of air, they are rejected. Finally, only symmetric regions are classified as bones.

III. RESULTS

The obtained relaxation maps are homogeneous (Figure 2), showing that the fitting model correctly compensates for the inhomogeneities of the B1-field yielding exact values. The figure 3 displays the obtained classification. Fat, muscle, prostate, air and background were correctly segmented and classified.

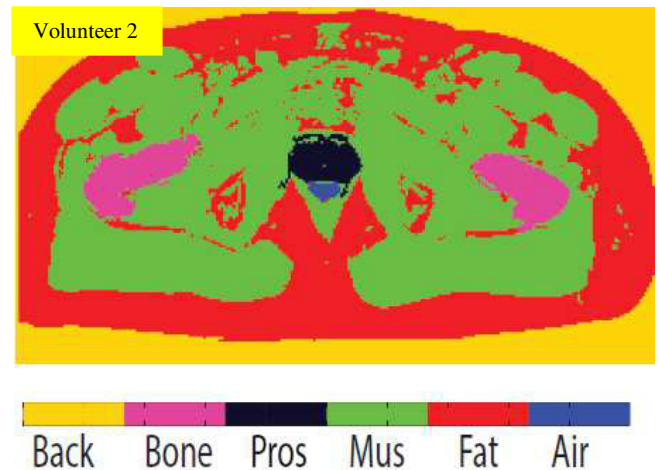


Figure 3: Classification of the different tissues at the level of the pelvis.

IV. DISCUSSION – CONCLUSION

In this work, we have proposed a new methodology for a first step to generate the attenuation correction map of PET/MRI systems for prostate imaging. Our approach correctly segments and classifies the attenuation-relevant structures used for this purpose (fat, air, background, bones and soft tissues). Big bones presented no problem and were accurately identified. However, small bones structures severely affected by partial volume effect were not efficiently detected. Nevertheless, the current results clearly demonstrate that the method could provide a first step to generate the attenuation map of PET/MRI systems in prostate imaging. The validation on a big data set is planned.

REFERENCES

- [1] H. Herzog, "PET/MRI: Challenges, solutions and perspectives," *Zeitschrift fur Medizinische Physik* 2010, Vol. 22, pp. 281–298.
- [2] K.-S. Chuang, H.-L. Tzeng, S. Chen, J. Wu, and T.-J. Chen, "Fuzzy c-means clustering with spatial information for image segmentation," *Computerized Medical, Imaging and Graphics*, 2006, vol. 30, pp. 9–15.